# NMR Self-Diffusion and Viscosity of Polyurethane Formulations for Rocket Propellants

**Kai F. Grythe, Finn K. Hansen,* and Harald Walderhaug**

*Department of Chemistry, University of Oslo, P.O. Box 1033 Blindern, N-0315 Oslo, Norway*

*Received: January 20, 2004; In Final Form: June 1, 2004*

Diffusion coefficients and viscosity have been measured in three different binary poly(urethane) binder formulations for solid rocket propellants. By means of the FT-PGSE NMR method the diffusion coefficients could be measured simultaneously for both the diisocyanate and prepolymer components with good accuracy. To calculate average diffusion coefficients for polydisperse substances, the stretched exponential function could be used successfully. The diffusion coefficients vary strongly with several orders of magnitude as a function of composition and also between the different systems from $5.04 \times 10^{-11}$ $m^2$ $s^{-1}$ for pure isophorone diisocyanate (IPDI) down to $9.34 \times 10^{-14}$ $m^2$ $s^{-1}$ for pure glyzidyl azide polymer (GAP). Plotted on a semilogarithmic scale against the prepolymer weight concentration, several of the diffusion coefficients show nearly linear behavior. Viscosities of these mixtures vary from 0.015 to 5.85 Pa s. An attempt to correlate the self-diffusion coefficients to the measured viscosity has been moderately successful. For all substances except GAP the self-diffusion coefficients scale close to the −0.6 power of the viscosity, according to the *quenched disorder* model. For GAP, the scaling factor is close to −0.9. While some systems can be explained quite well by a Rouse-type model, other systems cannot, the most important exception being the HTPB:IPDI system that shows phase separations at hydroxyl terminated polybutadiene (HTPB) concentrations below 50% w/w. The measured self-diffusion data have given valuable information for the interpretation of migration phenomena in rocket propellants.

## Introduction

Polyurethane is often used as a binder in the propellant matrix in a solid propellant rocket motor.[1] Solid rocket motors are insulated thin walled containers loaded with a solid propellant in which the most important ingredients are an oxidizer and a polymeric binder. In addition there are a number of additives such as plasticizer, catalyst(s), etc. One major area of concern in the production and storability of such motors is the adhesive bonding between the propellant and the casing insulation. Adhesion failure in the motor can lead to disastrous consequences. Because of the difference in chemical composition of the insulating material and the propellant, the adhesion properties between these components is a very sensitive function of the exact material compositions and processing variables such as time, temperature, etc. Some data have been reported on how to improve the adhesion between the propellant and the rocket case.[2−8] Schreuder-Gibson[5] gives a wide background of the adhesion problems in solid rocket motors. Of the more serious problems is migration of components across bondlines that can cause detrimental detoriation of bondline properties. This migration is often an issue with long-time storage of rocket motors, but migration, usually by a diffusive process, is also important in the production process of the motor. Diffusion in the polymer matrix before curing of the propellant is of major importance for the adhesion properties of the system, and in this context the diffusive processes can have both desired and undesired effects. The diffusion of components (e.g. prepolymers and/or curing agents) from the propellant into the insulation material is often a desired process, as it can result in bonding by polymer−polymer interpenetration in the final motor as predicted by the diffusion theory of adhesion.[9−12] However, this diffusion process may also affect the NCO/OH molar ratio in the curing poly(urethane) binder, leading to a region of a cohesively weaker propellant near the interface.[13] When a propellant is cast on to the insulation surface, the rate of diffusion of low molecular weight components into the insulation is most critical during the first hours of the curing of the binder. After the propellant is fully cured, the only mobile component left is usually the plasticizer. Even if long-term stability of the motor casting will be dependent on diffusion of this component, the diffusion during the initial curing period is expected to most strongly affect the strength of the bond.

The migration of components across the bondline is controlled by the mutual diffusion coefficients in the system and the relative solubility of the components in the two phases. In a homogeneous system consisting of n components, there will be $(n-1)^2$ different mutual diffusion coefficients connected to the n individual self-diffusion coefficients and thermodynamic properties of the components.[14] It is therefore in principle possible to predict mutual diffusion from self-diffusion data, but this is not a straightforward task. Yapel et al.[15] found that the Vrentas-Duda theory[16,17] successfully predicted mutual diffusion coefficients from self-diffusion coefficients of water in gelatin, but normally this theory needs many input parameters that are not easily obtained. In a heterogeneous composite system the diffusion coefficients will be furthermore affected by the obstruction caused by the filler particles even if the obstruction effect may be relatively easily calculated in moderately filled systems.[18] The measurement and calculation of diffusion coefficients in a complex composite system is therefore a formidable task.

* Corresponding author phone: (+47)22855554; fax: (+47)22855542; e-mail: f.k.hansen@kjemi.uio.no.

10.1021/jp049713k CCC: $27.50 
Published on Web 07/28/2004

**TABLE 1: $M_w$, $M_n$, and Polydispersity Index (PI) as Determined by GPC**

| substance | $M_w$ | $M_n$ | PI |
|---|---|---|---|
| GAP | 2818 | 2618 | 1.08 |
| HTPB | 9296 | 4628 | 2.01 |
| MDI | 568 | 327 | 1.73 |
| IPDI | 330.4 | 330.4 | 1.0 |

As a real rocket motor propellant is a complex composite system, this study is an initial attempt to obtain relevant data for the assessment of the mentioned migration processes. We have investigated a binder system consisting of the prepolymer and the curing agent, as we believe the obtained data will be relevant for the more realistic evaluation of the bonding mechanisms. As will be seen, there are differences of several orders of magnitude between diffusion properties of different prepolymers and curing agents, and this finding has already explained several observations in the bonded systems. In the literature studies of diffusion in systems consisting of hydroxyl terminated poly(butadiene) (HTPB) and isophorone diisocyanate (IPDI) are reported.[19−21] Meerwall et al.[19] found that the diffusion coefficient of the remaining unreacted curing agent (IPDI) is little affected by network formation, whereas the unreacted polymer molecules (HTPB) will be retarded. They also showed that the diffusion coefficients of both IPDI and HTPB, before any significant curing takes place, will increase with the concentration of IPDI, the latter acting like a plasticizer. In this study we have measured self-diffusion coefficients in uncured binary mixtures of two different prepolymers and two different diisocyanate curing agents by means of the Fourier transform pulse gradient spin−echo (FT-PGSE) NMR technique.[22] It is shown that by proper treatment of the NMR data, it is possible to simultaneously measure the self-diffusion coefficients of both components in the mixture. These data will then make the assessment of the mutual diffusion coefficient(s) more available. In addition we have measured the rheological properties of the mixtures, for the possible correlation between viscosity and self-diffusion. Such correlations will make extrapolation to other (unknown) systems easier.

## Experimental Section

**Chemicals.** Glyzidyl azide polymer (GAP) was obtained from SNPE propulsion. Hydroxyl terminated polybutadiene (HTPB), type R45M, was obtained from Elf Atochem. The HTPB has a *cis*-1.4/*trans*-1.4/vinyl-1,2 unsaturation ratio on 0.2:0.6:0.2. The molecular weights have been determined by gel-permeation chromatography (GPC), and the results are given in Table 1. 4,4′-Diphenylmethane diisocyanate (MDI) was obtained from Bayer and consists of a mixture of isomers and homologous components. Isophorone diisocyanate (IPDI) was obtained from Degussa, with the trade name VESTANAT IPDI. All chemicals were used as received.

All mixtures of prepolymer and diisocyanate were mixed by hand and evacuated for a few minutes in order to remove air bobbles. This preparation took about half an hour, and the measurements were started immediately after. All measurements were finished at a maximum of 2 h after the mixtures were made. This procedure was followed in order to avoid polymerization in the reactive systems.

**Fourier Transform Pulsed Gradient Spin−Echo NMR.** By measuring the change in spin−echo attenuation in a pulsed magnetic field gradient the molecular motion in a sample can be measured. The technique is widely described in the literature.[22−25] The method is applicable to polymer systems as mixtures, melts, rubbery networks and sols, colloidal suspensions, and emulsions.[26] In a typical Hahn echo FT-PGSE NMR experiment, the attenuation of the signals depends on the self-diffusion coefficient, $D$, of the investigated substance, and is given by the Stejskal-Tanner equation

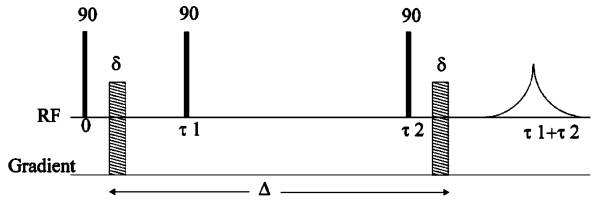


**Figure 1.** A stimulated echo is a result of three 90° RF pulses.

$$A_{(2\tau)} = A_{(0)} \exp\left(\frac{-2\tau}{T_2}\right) \exp\left[-(\gamma G\delta)^2\left(\Delta - \frac{\delta}{3}\right)\right] \quad (1)$$

where $\gamma$ is the magnetogyric ratio of the observed nucleus, $A_{(0)}$ and $A_{(2\tau)}$ are respectively the signal area immediately after and at time $2\tau$ after the 90° pulse, $T_2$ is the spin−spin relaxation time, and $G$ is the magnetic field gradient. In a Hahn pulse sequence (90°−180° radio frequency (RF) pulses) a magnetic field gradient is turned on for a time $\delta$ after an initial 90° RF pulse. At time $\tau$ there is a refocusing 180° RF pulse, and at time $\Delta$ after the first RF pulse the magnetic field gradient is turned on again for a time $\delta$. At time $2\tau$ the spin−echo has reached its maximum intensity, and the data acquisition starts. Fourier transformation of the second half of the echo gives the frequency resolved spectrum. In this work a modified version of the Hahn echo has been used, called the stimulated echo method.[22] The advantage of the stimulated echo method is that the observed echo attenuation is coupled with the spin−lattice relaxation $T_1$, rather than the spin−spin relaxation $T_2$. The $T_1$ relaxation time is often much longer than the $T_2$ relaxation time for polymers, which implies that the stimulated echo allows diffusion measurements using longer diffusion observation times. The method is therefore often better for measurement of low diffusion coefficients.

A stimulated echo is shown in Figure 1. The pulse sequence consists of a 90°-90°-90° three pulse sequence, and the attenuation of the signal area is given by

$$A_{(\tau_1+\tau_2)} = A_{(0)} 0.5 \exp\left(\frac{-(\tau_2-\tau_1)}{T_1} - \frac{2\tau_1}{T_2}\right) \exp\left[-(\gamma G\delta)^2\left(\Delta - \frac{\delta}{3}\right)\right] \quad (2)$$

If a system consists of only one type of molecules, only one single self-diffusion coefficient is observed. The signal attenuation ignoring constant relaxation effects may then be described by

$$\frac{A_{(\tau_1+\tau_2)}}{A_{(0)}} = \exp(-xD_S) \quad (3)$$

where

$$x = (\gamma G\delta)^2\left(\Delta - \frac{\delta}{3}\right) \quad (4)$$

A plot of $\ln((A/A_0))$ versus $(\gamma G\delta)^2(\Delta - (\delta/3))$ then renders a straight line. However, if the system consists of a distribution of different molecules, a distribution of diffusion coefficients should also be observed. From such a polydisperse system the

use of the empirical Kohlrausch−Williams−Watts (KWW) distribution function (also named a "stretched exponential") can be used to calculate a mean diffusion coefficient for the system.[27] Nyström et al.[28] found the KWW distribution to unequivocally represent data from this kind of systems. The signal attenuation may be described by

$$\frac{A_{(\tau_1+\tau_2)}}{A_{(0)}} = \exp[-(xD_{SE})^{\beta}] \quad (5)$$

that is a modified form of the Stejskal-Tanner equation. Here $x = (\gamma G\delta)^2(\Delta - (\delta/3))$ and $\beta$ is a parameter describing the width of the distribution of the diffusion coefficients. The parameter $\beta$ is constrained within the limits $0 \leq \beta \leq 1$, and if $\beta = 1$, eq 5 simplifies to eq 3. The value of $\beta$ will decrease with the increasing width of the distribution of diffusion coefficients. $D_{SE}$ is related to the self-diffusion coefficient, $D_S$, in the following way[27]

$$\frac{1}{D_S} = \int_0^{\infty} \exp[-(xD_{SE})^{\beta}]dx = \frac{1}{\beta}\Gamma\left(\frac{1}{\beta}\right)\frac{1}{D_{SE}} \quad (6)$$

Here, $\Gamma$ is the gamma function. It should be noted that the mean value of $D_S$ calculated this way is an average over $1/D_{SE}$ and not $D_{SE}$ itself, according to eq 6.[29] It is also possible to fit data sets with combinations of eqs 3 and 4. If a system consists of two different components, one that shows a single-exponential behavior (denoted with (1)) and one that has a stretched exponential behavior (denoted with (2)), the system can be fitted with the equation

$$\frac{A_{(\tau_1+\tau_2)}}{A_{(0)}} = (1 - B)\exp(-xD_{S(1)}) + B\exp[-(xD_{SE(2)})^{\beta}] \quad (7)$$

where $B$ is a weighting parameter. Several combinations of exponential functions may be constructed in this way but requires that there are sufficient and accurate data for the curve fit. With an increasing number of fitted parameters, there is also the danger of obtaining physically unrealistic parameters. We have therefore not ventured into these possibilities any further.

All measurements have been carried out on a Bruker CXP 200 spectrometer equipped with a proton field gradient probe from Cryomagnetics Inc. The system is capable of producing gradients up to 800 T $m^{-1}$. Experiments were done by measuring $A$ as a function of $G$. The values for $\delta$ and $\Delta$ have been adjusted to give the best attenuation of the echo signal, and typical values for $\Delta$ are 140−300 ms and for $\delta$ 2−3 ms. To avoid thermally induced convection currents in the sample, all measurements were carried out at ambient temperature that was 19 °C. The temperature was measured in a separate sample by means of the chemical shift of ethylene glycol and was assumed constant for all measurements.

**Rheology.** All rheology measurements were performed on a Bohlin VOR rheometer equipped with either 14 mm concentric cylinders or a double gap measuring systems. Two different torsion bars were used to optimize stress detection. As all the measured substances show Newtonian rheologic behavior, the shear rates were varied in order to optimize sensitivity and reproducibility. The shear rates used were in the range of 0.05−50 $s^{-1}$. The instrument was calibrated with a viscosity standard. All measurements were conducted at 19 ± 0.5 °C, measured directly in the samples. The reproducibility of these measurements was ca. 3%.

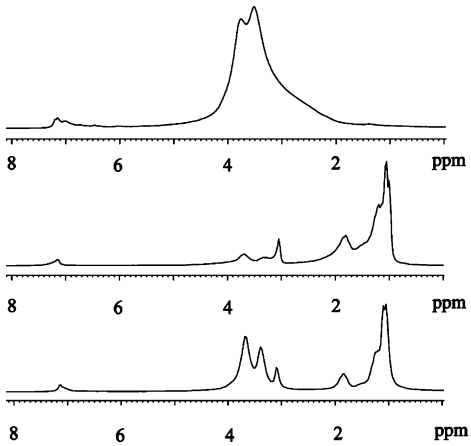


**Figure 2.** NMR spectra of (from the top) pure GAP, pure IPDI, and a 1/1 w/w mixture of GAP and IPDI.

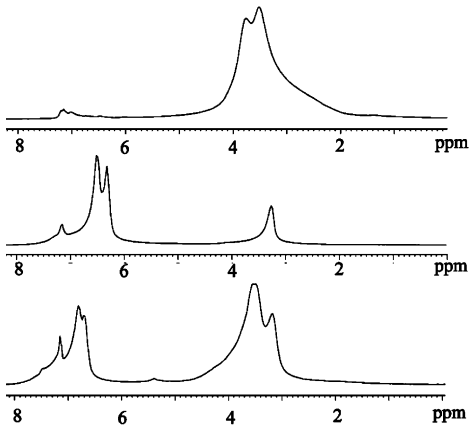


**Figure 3.** NMR spectra of (from the top) pure GAP, pure MDI, and a 1/1 w/w mixture of GAP and MDI.

## Results

**NMR Self-Diffusion.** The self-diffusion coefficients were measured by FT-PGSE NMR in both pure substances and in mixtures of prepolymers and diisocyanates. The three investigated systems were GAP:IPDI, GAP:MDI, and HTPB:IPDI. Before presenting the results we will consider the errors involved in the measurements. The errors in sample concentrations are considered to be negligible, amounting to a maximum 0.3%. However, the determined diffusion coefficients may contain larger errors, stemming both from the method of integration, the ability to separate the different signals, and possible temperature variations. If a signal is composed of two different signals, the influence of the two signals will vary with the composition. The information in a low intensity signal will be more prone to errors than that in a high-intensity signal. It is therefore believed that the error is larger at small concentrations. If the low intensity signal is well separated from other signals, the error may be small, but low intensity signals not well separated from other signals may contain larger errors.

In Figure 2 NMR spectra of pure GAP, pure IPDI, and a 1/1 w/w mixture of GAP and IPDI are shown. The signal at 7.15 ppm is benzene, which is used as reference. In the 1/1 mixture spectrum, there is a cluster of 3 signals at 3−4 ppm. The two large signals are from GAP, and the small signal is from IPDI. In Figure 3 NMR spectra of pure GAP, pure MDI, and a 1/1 mixture of GAP and MDI are shown. The signal at 7.15 ppm is the benzene reference. In the 1/1 mixture, the benzene signal is a shoulder on the MDI signal. The GAP signal at 2.8−4.5

**TABLE 2: Data from FT-PGSE NMR Measurements and Viscosity of the Single Components.**

| substance | method | $D_{SE}$ ($m^2s^{-1}$) | 80% CI ($m^2s^{-1}$) | $b$ | $D_S^0$ ($m^2s^{-1}$) | $\eta$ (Pa s) |
|---|---|---|---|---|---|---|
| GAP | stretched exp. | $9.66 \times 10^{-14}$ | $9.65-9.66 \times 10^{-14}$ | 0.93 | $9.34 \times 10^{-14}$ | 5.85 |
| HTPB | stretched exp. | $1.70 \times 10^{-13}$ | $1.695-1.697 \times 10^{-13}$ | 0.78 | $1.48 \times 10^{-13}$ | 8.44 |
| MDI | stretched exp. | $4.34 \times 10^{-12}$ | $4.33-4.34 \times 10^{-12}$ | 0.84 | $3.95 \times 10^{-12}$ | 0.54 |
| IPDI | single exp. | $5.04 \times 10^{-11}$ | $4.99-5.07 \times 10^{-11}$ | 1 | $5.04 \times 10^{-11}$ | 0.0152 |

ppm in the mixture also contains a signal from MDI. In Figure 4 NMR spectra of pure HTPB, pure IPDI, and a 1/1 mixture of

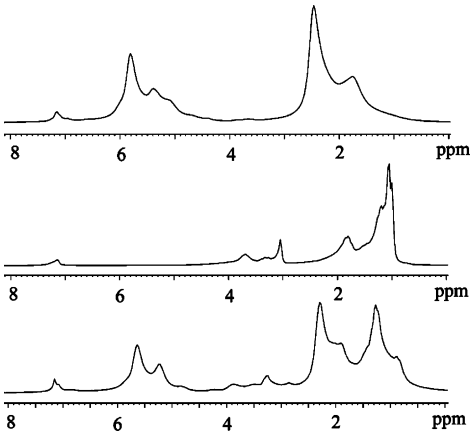


**Figure 4.** NMR spectra of (from the top) pure HTPB, pure IPDI, and a 1/1 w/w mixture of HTPB and IPDI.

HTPB and IPDI are shown. The signal at 7.15 ppm is the benzene reference. In the 1/1 mixture spectrum it is easy to recognize the signal at 5−6 ppm from HTPB. The other signal from HTPB and the main signal from IPDI are overlapping in the mixture spectrum.

All processing of the FT-PGSE data has been done with the Component-Resolved (CORE) NMR spectroscopy software, developed by Stilbs and co-workers.[30−32] CORE is a new data processing mode for FT-PGSE data sets. The procedure is based on a global least-squares minimization approach. In contrast to conventional analysis this method utilizes all spectral information, resulting in an enhancement of signal-to-noise ratio by a factor of 10 or more.[30] CORE is particularly useful is systems with overlapping band shapes and high dynamic range with regard to constituent spectral intensities. As an alternative method, data processing by integration of the different band shapes and a subsequent nonlinear curve fit of the band shape areas was also performed. The results from this processing agree to a large extent with the CORE results for both overlapping and nonoverlapping band shapes, but the CORE method was preferred, as the results for partly overlapping band shapes were better.

In Figure 5a−e the graphical output from CORE for a 1/1 mixture of GAP and MDI are shown. Figure 5a shows the FT-PGSE spectrum, the CORE fit to this data set is shown in Figure 5b, and the difference spectrum between these two is shown in Figure 5c. As seen, the fit is quite good, and there seems to be little systematic error. Figure 5d,e shows how the CORE fit divided the spectrum into the two different components.

If an unassociated system consists of only one type of molecules, only a single diffusion coefficient should be observed. However, if the system is sufficiently polydisperse with regard to molecular weight, a distribution of diffusion coefficients may be observed. In all the systems investigated, only IPDI shows one single diffusion coefficient, consistent with it being single molecular species. The results for GAP, HTPB, and MDI were fitted to stretched exponential functions (KWW functions), even though the polydispersity of GAP was quite low (1.08, Table 1). Stilbs et al.[30] state that good initial estimates of the self-diffusion coefficients are not required for the minimization to work. However, we found that in more complex models than a single-exponential function, good initial estimates were indeed necessary for convergence of the CORE procedure. These estimates were found from a conventional integration and subsequent nonlinear analysis and fit (using the Origin program) of the signal attenuation to the suggested model. It is possible that a single exponential fit by using CORE probably also would have given satisfactory initial estimates.

The conventional integration and subsequent nonlinear analysis and fit also was used for two samples in the GAP:MDI series, where the CORE analysis failed. In this method the FT-PGSE NMR signal was integrated in XWINNMR and imported into the ORIGIN software. From the plots of the signal attenuation as a function of the gradient strength the data were fitted to the appropriate model. As MDI is not monodisperse, the MDI signal is fitted to eq 5. The data points at intensities below ca. 10% are neglected as they are most likely influenced by noise and also of the GAP signal. The GAP signal was also fitted to eq 5. This signal also contains an MDI signal and increasingly so at higher MDI concentrations. For all mixtures except low GAP concentrations, the MDI signal attenuates about 10 times faster than the GAP signal, and therefore only the first few data points will be affected by the disturbance from MDI. Instead of leaving the noise from MDI as an error, it should in principle be possible to extract the diffusion coefficient of both MDI and GAP by fitting a double stretched exponential function. Unfortunately, this procedure did not give reproducible results, since the diffusion coefficients for GAP and MDI are too similar. Another reason may be that the GAP signal is too large compared to the MDI signal, so the contribution from MDI may actually be neglected.

The results from measurements of the pure substances are given in Table 2. In this table both self-diffusion coefficients and viscosities are given for easy comparison. At first sight the self-diffusion coefficients are not well correlated with the molecular weights as given in Table 1. The self-diffusion coefficient for GAP is lower than that of HTPB, even if GAP has the lower molecular weight. Also the value for MDI is much lower than for IPDI, even if these substances have similar $M_n$. However, the differences in molecular weight distributions may explain parts of these discrepancies, and the correlation of self-diffusion coefficients with viscosities seem to be better. These findings will be further discussed below. The 80% confidence interval is calculated by a Monte Carlo-based parameter error estimation integrated in CORE.

In Figures 6−8 the diffusion coefficients are plotted against the concentration of the prepolymers. Figure 6 shows the self-diffusion coefficients for GAP and IPDI in the GAP:IPDI mixtures as a function of GAP concentration. The diffusion coefficients of both GAP and IPDI are decreasing with increasing GAP concentration. Plotted on a logarithmic $y$-axis, the data points seem quite linear and have therefore been fitted to straight lines. For IPDI it is seen that the fitted line intercepts the $y$-axis at a higher $D$ than the measured self-diffusion coefficient of

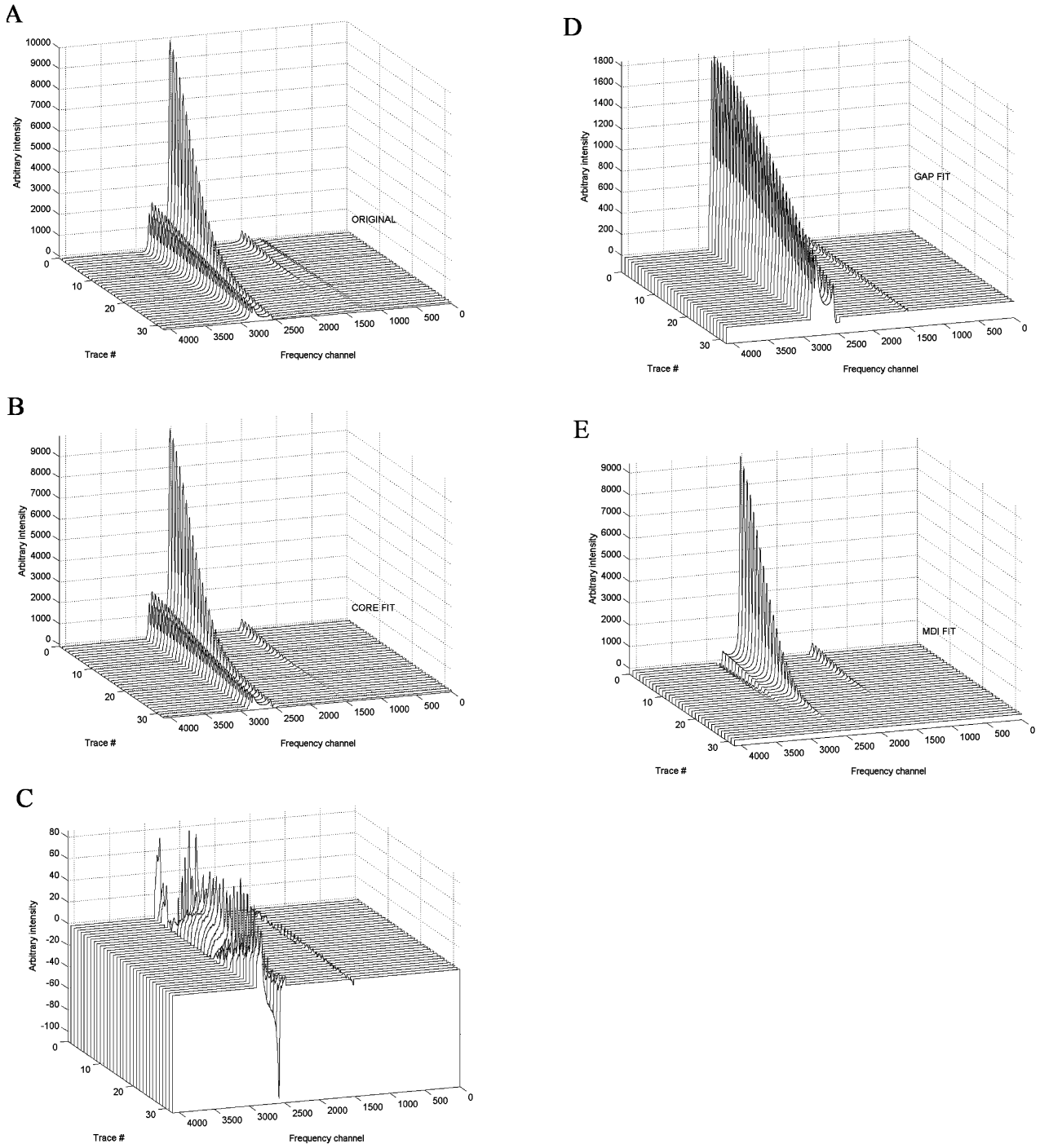


**Figure 5.** (a) Sequence of FT-PGSE spectra for a 1/1 mixture of GAP and MDI at 19 °C. Peak amplitudes reflect the values of the self-diffusion coefficients of the individual constituents according to the Stejskal-Tanner relation. (b) CORE fit to the data set. (c) Residuals. (d) CORE fit of the GAP component. (e) CORE fit of the MDI component.

pure IPDI, but this fact is hardly significant, as a closer inspection reveals that the plot of the data points in reality is slightly curved. Figure 7 shows the self-diffusion coefficients for GAP and MDI in the GAP:MDI mixtures as a function of GAP concentration. The plot for MDI on the logarithmic *y*-axis is also quite linear but contains somewhat more noise than the plot for IPDI in Figure 6. As in Figure 6 the fitted line intercepts the *y*-axis at a higher *D* than the self-diffusion coefficient of pure MDI showing that this plot is also slightly curved. The self-diffusion coefficient of GAP exhibits a clearer nonlinear behavior. Some of this behavior may be due to artifacts stemming from the confounding of the GAP signal by the MDI signal as seen from Figure 3. This effect will be more evident at lower GAP concentrations where the MDI signal is stronger. The two lowest points, at 12 and 18% GAP concentration, was calculated using the conventional integration procedure, as even the CORE program failed with this data set. This may well explain the larger deviation in the two points at low GAP concentration. One would expect, however, that the diffusion coefficient of GAP would be closer to that of MDI at low GAP concentrations because the molecular weight of GAP is only ca. 5 times that of MDI. Figure 8 shows the self-diffusion coefficients for HTPB and IPDI in the HTPB:IPDI mixtures as a function of HTPB concentration. There are no measurements between 0 and 50% HTPB as HTPB and IPDI are not miscible at these concentrations. If the IPDI data points are extrapolated

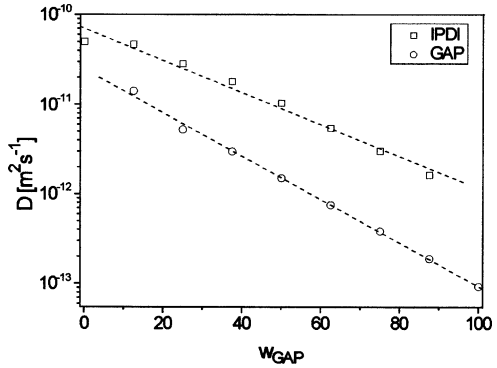


**Figure 6.** The self-diffusion coefficient of IPDI and GAP as function of the GAP content.

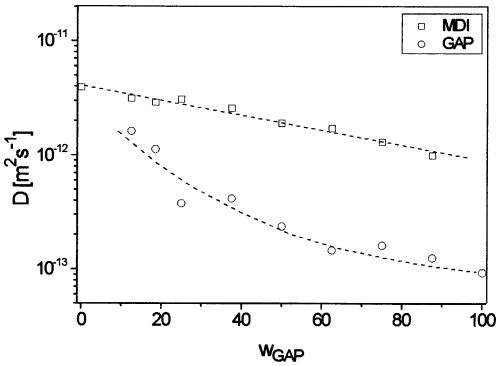


**Figure 7.** The self-diffusion coefficient of MDI and GAP as function of the GAP content.

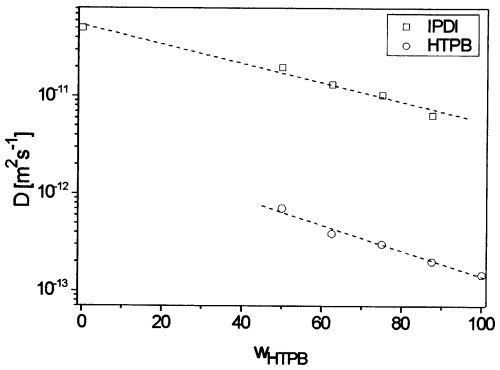


**Figure 8.** The self-diffusion coefficient of IPDI and HTPB as function of the HTPB content.

by a fitted straight line to 0% HTPB, the value is seen to coincide well with the value of $D_S$ of pure IPDI.

**Rheology.** The viscosity of all mixtures in the NMR study was measured. With these measurements precautions were taken to avoid polymerization of the reactive mixtures, as described in the Experimental Section. As with the NMR measurements, all viscosity measurements were finished in a maximum of 2 h after the mixtures were made. At room temperature and without any curing catalyst the rate of reaction is considerably less than under ordinary curing conditions. To verify this assumption, viscosity was measured as a function of time during the first 3 h after mixing in 3 samples containing about 13% curing agent. In the HTPB:IPDI and the GAP:MDI systems, the viscosity increased a few percent, and in the GAP:IPDI system a small decrease in viscosity was observed. This is most likely caused by temperature variations (temperature increased 1.3 °C during this measurement) or by drift in the instrument. It was therefore concluded that polymerization did not influence the FT-PGSE diffusion results.

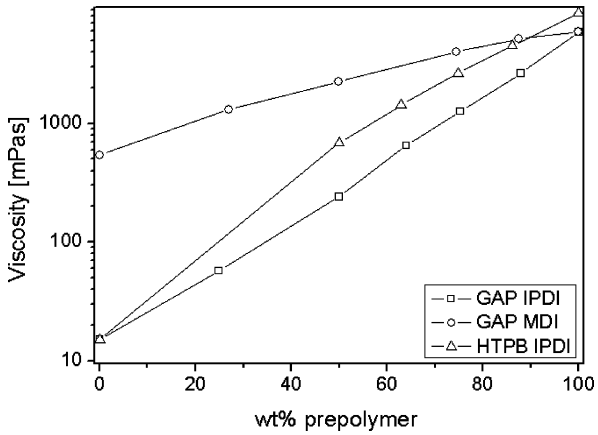


**Figure 9.** The viscosity as a function of prepolymer content. All measurements at 19 °C.

All samples were measured at 19 ± 0.5 °C in order to be comparable to the NMR measurements. Temperature control is very important in these systems, especially in the highest viscosity samples, as in HTPB a temperature increase of 1 °C will increase the viscosity 6%. Measured viscosities are therefore considered to be within ±3%.

The results from the viscosity measurements are shown in Figure 9. The missing data from the HTPB:IPDI system below 50% HTPB are due to phase separation in this range, as already mentioned. The obvious difference between the MDI containing system and the other two is due to the much higher viscosity of MDI itself, probably caused by of its content of higher molecular weight homologues.

## Discussion

The shapes of the semilogarithmic plots of the self-diffusion coefficients as a function of polymer concentration are interesting in several ways. First, several of the plots are near linear over the whole concentration range. There is no available theory that directly predicts this behavior, and as the linearity (i.e. single exponential dependency) at closer inspection is not always perfect, the fact does not lend itself to easy interpretation. However, the near linearity is useful both for interpolation and extrapolation of the self-diffusion coefficients to infinite dilution. This is feasible for the low molecular weight diisocyanates in all systems and GAP in the GAP:IPDI system. It is difficult for GAP in the GAP:MDI system and not possible in the HTPB:IPDI system because of the phase separation. For all but the latter system it is observed that linearity of the semilogarithmic plots are best at lower concentrations of the opposite component. This means that we can generally express the self-diffusion data by means of a simple exponential relationship given by

$$D_1 = D_1^{\,0} \exp(a w_2) \tag{8}$$

where $D_1$ is the self-diffusion coefficient of any component in the mixture, $D_1^{\,0}$ is the corresponding value of the pure component (given in Table 2), and $w_2$ is the weight fraction of the other component ($w_2 = 1 - w_1$). The exponent, $a$, is thus a characteristic constant for the binary mixture within a certain concentration range. This constant has been determined for all the systems by linear regression, and the values are presented in Table 3.

Second, the three plots (Figures 6−8) are distinctly different. Most interesting is maybe that the ratio between the two self-diffusion coefficients in the GAP systems is ca. 10 at high

**TABLE 3: Values for the Exponent *a* in Eq 8 for All the Investigated Systems[a]**

| system | *a* | validity range |
|---|---|---|
| IPDI in GAP | $-2.96 \pm 0.37$ | $w_2 < 0.9$ |
| MDI in GAP | $-1.23 \pm 0.21$ | $w_2 < 0.6$ |
| IPDI in HTPB | $-2.08 \pm 0.12$ | $w_2 < 0.9$ |
| GAP in IPDI | $6.79 \pm 0.44$ | $w_2 < 0.9$ |
| GAP in MDI | $1.70 \pm 0.41$ | $w_2 < 0.6$ |
| HTPB in IPDI | $3.46 \pm 0.33$ | $w_2 < 0.6$ |

[a] The error given is the standard deviation.

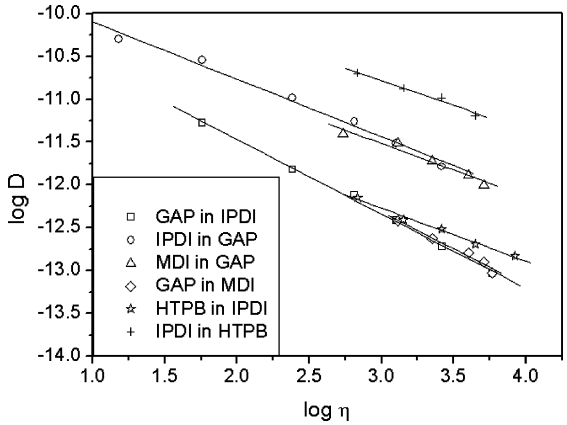


**Figure 10.** Plot of log(D) versus log($\eta$) for both components in the 3 different mixtures. The straight lines are fitted by linear regression.

prepolymer concentrations, while it for the HTPB system is ca. 50. This difference is probably caused by the higher molecular weight of HTPB compared to that for GAP but may in addition be connected to the lower interaction between HTPB and IPDI, resulting in phase separation at some concentrations. These differences will be further discussed below.

The objective of this work is to assess the magnitude of diffusion processes in the binary mixtures that constitute poly(urethane) prepolymers. The mutual diffusion coefficient for the binary mixture, $D_{12}$, is connected to the separate self-diffusion coefficients and may in principle be calculated from these, but this is not a straightforward procedure. Many different expressions have been proposed, one of the simplest being[14]

$$D_{12} = B_2^x(x_2 D_1 + x_1 D_2) \tag{9}$$

where

$$B_2^x = \frac{1}{RT}\left(\frac{\partial \mu_2}{\partial \ln x_2}\right)_{T,p} = 1 + \left(\frac{\partial \ln f_2}{\partial \ln x_2}\right)_{T,p} \tag{10}$$

is the thermodynamic factor. Here $D_i$ are the individual self-diffusion coefficients, $x_i$ are the mol fractions of each component, $\mu_2$ is the chemical potential, and $f_2$ is the rational activity coefficient of component 2. This equation is also known as the Darken equation and has been widely used, but it has some limitations. It does, however, represent the limiting behavior expected for the mutual diffusion coefficient at each end of the concentration scale. When either $x_1$ or $x_2$ approaches zero, $B_2^x \rightarrow 1$, and $D_{12}$ is then given by the extrapolated self-diffusion coefficient of the respective component at infinite dilution in the other component. For a polymeric system, $B_2^x$ might be calculated by the Flory−Huggins theory, but missing the interaction parameter in this theory, we have not attempted this. In addition, the linear dependence of $D_{12}$ on $B_2^x$ has also been debated, so there is a question of the justification of such a procedure. Because a normal mix for a poly(urethane) is usually made at an approximately equimolar ratio ($x_1 = x_2 = 0.5$), we may anticipate that in the cases where $D_1 \gg D_2$, the value of $D_{12}$ will be most close to $D_1$.

**TABLE 4: Slope ($-\xi$) of the Plot of Self-Diffusion Coefficients, $D_S$, against Viscosity $\eta$ of the Mixture[a]**

| system | $\xi$ |
|---|---|
| GAP in IPDI | $0.87 \pm 0.02$ |
| IPDI in GAP | $0.67 \pm 0.04$ |
| MDI in GAP | $0.62 \pm 0.08$ |
| GAP in MDI | $0.86 \pm 0.08$ |
| HTPB in IPDI | $0.62 \pm 0.04$ |
| IPDI in HTPB | $0.58 \pm 0.06$ |

[a] The error given is the standard deviation.

The correlation between self-diffusion and viscosity is often discussed, but good general theories giving quantitative agreement for all types of molecules are not found.[14] The simplest of these theories is described by the Stokes−Einstein (S−E) equation. It is restricted to the movement of spherical particles at low concentrations in a continuum of smaller molecules. The diffusion coefficient is given by

$$D = \frac{kT}{6\pi\eta a} \tag{11}$$

where $a$ is the radius of the spherical particles, and $k$ is Boltzmann's constant. For the diffusion of molecules, especially in more concentrated solutions, this equation is often incorrect even for small molecules.[14] The dependence of $D$ upon $\eta$ can be evaluated by plotting them on a double logarithmic scale as shown in Figure 10. The slopes of the curves are given in Table 4.

As seen in Figure 10 the data may be classified into 3 distinct groups that at high viscosities have diffusion coefficients around $10^{-11}$, $10^{-12}$, and $10^{-13}$, respectively. The two first groups consist of the two low molecular weight diisocyanates, while the last group consists of the two prepolymers. That the prepolymers have lower diffusion coefficients is expected, but it is surprising that $D_S$ for HTPB is slightly higher than for GAP at high viscosities despite the higher molecular weight of HTPB. The reason for this is probably the difference in attractive interaction between GAP:IPDI and HTPB:IPDI. In the latter system the interaction is clearly less favorable, leading to phase separation at some molar ratios. This lack of attractive interaction can lead to a higher self-diffusion coefficient of IPDI. The slopes given in Table 4 are those of the so-called Fractional Stokes−Einstein (FSE) equation:[33]

$$D = C\eta^{-\xi},\ 0 < \xi \leq 1 \tag{12}$$

This is an empirical equation found to describe tracer diffusion in many polymer systems. The exponent, $\xi$, is in the range 0.5−0.9 for several systems. The deviation from the SE equation has been explained by the development of heterogeneities and particle clustering in glass-forming liquids and has been named the *quenched disorder* model by Douglas.[34] He has derived a theoretical value of $\xi = 3/5$ for a model fluid containing idealized obstructing spheres. It is interesting to note that this value is close to the one we have found for the HTPB:IPDI system (both HTPB in IPDI and opposite) and for IPDI and MDI in the GAP mixtures. It therefore seems as the first system follows the quenched disorder model well. Only GAP in the latter two systems deviates significantly, with a higher exponent around 0.9 for both systems. Douglas explains other exponents as a result of deviations from spherical configuration,

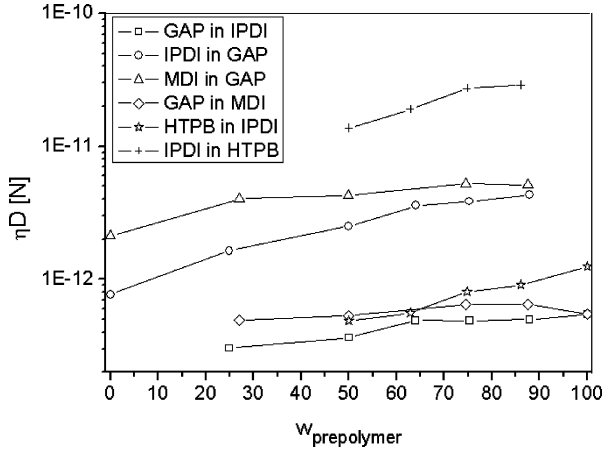


**Figure 11.** The product $\eta D$ as a function of prepolymer concentration for both components in the 3 different mixtures.

so this may be the reason for the deviation of the GAP polymer. All in all, the results look quite satisfactory for predictive purposes.

According to the SE equation the product $\eta D$ is constant and only dependent on the size of the diffusing molecules. Deviations from this constancy are often used to discuss nonideality.[14] The Rouse model is often used to predict viscous and diffusive behavior for unentangled low molecular weight polymers.[35] In the Rouse model the diffusion coefficient and the viscosity are given by

$$D_{\text{Rouse}} = \frac{kTM_0}{\zeta M} \tag{13}$$

$$\eta_{\text{Rouse}} = \frac{\rho\zeta N_a \langle R_G^2 \rangle}{6M_0} \tag{14}$$

In eqs 13 and 14 $M_0$ is the monomer molecular weight, $\zeta$ is the monomeric friction factor, $\rho$ is the density, $M$ is the polymer molecular weight, and $\langle R_G^2 \rangle$ is the mean square radius of gyration. The problem with predicting $D$ and $\eta$ from the Rouse model is how to handle the friction factor. However, the product $\eta D$ is independent of the monomeric friction factor. Hence from eqs 13 and 14

$$(\eta D)_{\text{Rouse}} = \frac{\rho RT \langle R_G^2 \rangle}{6M} \tag{15}$$

Pearson et al.[35,36] have found this product to be constant for $M$ less than 5000 for a linear polyethylene. When $M$ reaches a certain value the product of $\eta D$ will start to increase, due to entanglements. This behavior is described by the reptation model, but the molecular weights of the investigated systems are probably too low for entanglements.

In Figure 11 the product $\eta D$ has been plotted against the prepolymer concentration. The three different groups mentioned above are again clearly distinguishable. The lower group contains the two polymers, and the product $\eta D$ is almost constant, except that the data for HTPB are increasing somewhat above that of GAP. The two curves for GAP are almost identical, and this prepolymer follows eq 15 well. The value for $\eta D = 5 \times 10^{-13}$ results in a value of $R_G = 1.9$ nm that seems quite reasonable. The value of $R_G$ for HTPB increases with concentration, if eq 15 is to be interpreted for this prepolymer. Because of the higher molecular weight of HTPB, the same value of $\eta$D as for GAP gives $R_G = 2.5$ nm. The middle group consists of the two diisocyanates in GAP. For these $\eta D$ is not quite constant but is more so for MDI than IPDI. A value of $3 \times 10^{-12}$ for $\eta$D gives $R_G = 1.6$ nm for MDI. If the increasing trend in the curve for IPDI is to be interpreted in the same way, it means that $R_G$ should increase with GAP concentration. It is, however, not certain that these data can be interpreted strictly according to the Rouse model, and other effects may be causing this increase. These questions arise more so for the upper curve, IPDI in HTPB. According to eq 15, it would appear that $R_G$ is still higher for IPDI in HTPB than in GAP and should increase with increasing HTPB concentration. Even if the latter fact may be possible, the interpretation of these data according to the Rouse model seems doubtful, especially on the background of unfavorable interactions. If the chain collapses, the molecule becomes smaller, and this will explain a higher diffusion coefficient. It would be necessary to obtain more thermodynamic data for this system in order to explain it better.

## Conclusions

It is possible to measure the diffusion coefficients of both the diisocyanate and the prepolymer in these systems with good accuracy. To calculate average diffusion coefficients for polydisperse substances, the stretched exponential function can be used successfully. The diffusion coefficients vary strongly with several orders of magnitude as a function of composition and also between the different systems from $5.04 \times 10^{-11}$ ms$^{-2}$ for pure IPDI down to $9.34 \times 10^{-14}$ ms$^{-2}$ for pure GAP. The mutual diffusion coefficients in these systems has not been measured, but in the most commonly used 1/1 molar ratio it is believed that these are relatively close (within 50%) to the values of the diisocyanates. This will explain observations on similar systems used as binders for solid rocket propellants, where migration of components across the interfaces during the production process has been recognized as a problem. With a diffusion coefficient of $10^{-11}$ ms$^{-2}$ a component can diffuse an average distance of 0.27 mm in 1 h, while at $10^{-13}$ ms$^{-2}$ the distance is only 1/10 of this value. Formulations that lower the diffusion rates are therefore desirable.

The attempt to correlate the self-diffusion coefficients to viscosity in these systems has been moderately successful. While some systems can be explained quite well by a Rouse-type model, other systems cannot, the most important exception being the HTPB:IPDI system that shows phase separations at HTPB concentrations below 50% w/w. For this technically important system better thermodynamic understanding might still be needed.

The HTPB:IPDI system (both HTPB in IPDI and opposite) and IPDI and MDI in the GAP mixtures follow the *quenched disorder* model quite well. Only GAP deviates significantly which can be explained as a result of deviations from spherical configuration.

**Acknowledgment.** We wish to thank Professor Eddy W. Hansen at the Department of Chemistry, University of Oslo for valuable help with the NMR measurements and Torbjørn Olsen at the Norwegian Defense Research Establishment for general help with chemicals and discussions. We also wish to thank the Norwegian Defense Research Establishment and NAMMO Raufoss for financial support.

## References and Notes

(1) *Solid Rocket Propulsion Technology*; Davenas, A., Ed.; Pergamon Press: Oxford, 1993.

(2) Haska, S. B.; Pekel, F. *International Annual Conference of ICT* **1995**, *26th*, 49/1.
(3) Haska, S. B.; Bayramli, E.; Pekel, F.; Ozkar, S. *J. Appl. Polym. Sci.* **1997**, *64*, 2355.
(4) Sanden, R.; Wingborg, N. *J. Appl. Polym. Sci.* **1989**, *37*, 167.
(5) Schreuder-Gibson, H. L. *Rubber World* **1990**, *203*, 34.
(6) Gottlieb, L.; Bar, S. *Propellants, Explosives, Pyrotechnics* **2003**, *28*, 12.
(7) Giants, T. W. *Case bond liner systems for solid rocket motors*; Mater. Sci. Lab., Aerosp. Corp., El Segundo, CA, U.S.A. FIELD URL:, 1991.
(8) Hemminger, C. S. *Surface Characterization of Solid Rocket Motor HTPB Liner Bond System*; 33rd AIAA/ASME/SAE/ASEE Joint Propulsion Conference & Exhibit, 1997, Seattle, WA.
(9) Voyutskii, S. S.; Vakula, V. I. *Rubber Chem. Technol.* **1964**, *37*, 1153.
(10) Jabbari, E.; Peppas, N. A. *J. Macromol. Sci., Rev. Macromol. Chem. Phys.* **1994**, *C34*, 205.
(11) Pocius, A. V. *Adhesion and adhesives technology: An introduction*; Hanser: München, 2002.
(12) Ruch, F.; David, M. O.; Vallat, M. F. *J. Polym. Sci., Part B: Polym. Phys.* **2000**, *38*, 3189.
(13) Grythe, K. F. *Study of the interface between insolation and propellant in solid propellant rocket motors*; NTNU, 2002.
(14) Tyrell, H. J. V.; Harris, K. R. *Diffusion in Liquids*; Butterworth: London, 1984.
(15) Yapel, R. A.; Duda, J. L.; Lin, X.; von Meerwall, E. D. *Polymer* **1994**, *35*, 2411.
(16) Vrentas, J. S.; Duda, J. L. *J. Polym. Sci. B.; Polym. Phys.* **1977**, *15*, 403.
(17) Vrentas, J. S.; Duda, J. L. *J. Polym. Sci. B.; Polym. Phys.* **1977**, *15*, 417.
(18) Amsden, B. *Macromolecules* **1999**, *32*, 874.
(19) von Meerwall, E. D.; Palunas, P. *J. Polym. Sci., Part B: Polym. Phys.* **1987**, *25*, 1439.
(20) von Meerwall, E. D.; Stone, T. *J. Polym. Sci., Part B: Polym. Phys.* **1989**, *27*, 503.
(21) Tao, H.; Lodge, T. P.; von Meerwall, E. D. *Macromolecules* **2000**, *33*, 1747.
(22) Stilbs, P. *Prog. NMR Spectrosc.* **1987**, *19*, 1.
(23) Von Meerwall, E. D. *Adv. Polym. Sci.* **1984**, *54*, 1.
(24) Peppas, N. A.; Korsmeyer, R. W. *Polym. News* **1985**, *10*, 265.
(25) Masaro, L.; Zhu, X. X. *Can. J. Anal. Sci. Spectrosc.* **1998**, *43*, 81.
(26) Von Meerwall, E. D. *J. Non-Cryst. Solids* **1991**, *131*−*133*, 735.
(27) Walderhaug, H.; Hansen, F. K.; Abrahmsen, S.; Persson, K.; Stilbs, P. *J. Phys. Chem.* **1993**, *97*, 8336.
(28) Nystrom, B.; Walderhaug, H.; Hansen, F. K. *J. Phys. Chem.* **1993**, *97*, 7743.
(29) Stilbs, P. *Surf. Sci. Ser.* **1998**, *77*, 239.
(30) Stilbs, P.; Paulsen, K.; Griffiths, P. C. *J. Phys. Chem.* **1996**, *100*, 8180.
(31) Stilbs, P.; Paulsen, K. *Rev. Sci. Instrum.* **1996**, *67*, 4380.
(32) Stilbs, P. *J. Magn. Reson.* **1998**, *135*, 236.
(33) Douglas, J. F.; Leporini, D. *J. Non-Cryst. Solids* **1998**, *235*−*237*, 137.
(34) Douglas, J. F. *Comput. Mater. Sci.* **1995**, *4*, 292.
(35) Pearson, D. S.; Fetters, L. J.; Graessley, W. W.; Ver Strate, G.; von Meerwall, E. *Macromolecules* **1994**, *27*, 711.
(36) Pearson, D. S.; Ver Strate, G.; Von Meerwall, E.; Schilling, F. C. *Macromolecules* **1987**, *20*, 1133.